Correlation-based phase noise measurements

Enrico Rubiola* Vincent Giordano†

Cite this article as:
E. Rubiola, V. Giordano, "Correlation-based phase noise measurements",
Review of Scientific Instruments vol. 71 no. 8 pp. 3085–3091, August 2000

Abstract

In the characterization of the phase noise of a component, it is common practice to measure the cross spectrum density at the output of two phase detectors that simultaneously compare the component output signal to a common reference. This technique, which is based on correlation and averaging, allows the rejection of the phase detector noise. On the other hand, it is known that the interferometer exhibits lower noise floor and higher conversion gain than other phase detectors suitable to radiofrequency and microwave bands. Thus, we experimented on an improved instrument in which the phase noise of a component is measured by correlating and averaging the output of two interferometers. The measurement sensitivity, given in terms of noise floor, turns out to be limited by the temperature uniformity of the instrument, instead of the absolute temperature T. This feature makes the instrument suitable to investigate the spectrum $S_\varphi(f)$ of phase fluctuations below k_BT/P_o, i.e. the thermal energy k_BT referred to the carrier power P_o. The described method is suitable to the implementation of instruments in a wide frequency range, from some 100 kHz to 40 GHz and beyond. In principle, this method can also be exploited for the measurement of amplitude noise. Theory and experimental proof are given.

Contents

1 Introduction **1**

2 Basic Concepts **3**

3 The Phase Noise Measurement System **6**

4 Signal Analysis of the Double Interferometer **6**

*Université Henri Poincaré, Nancy, France, e-mail `enrico@rubiola.org`
†Dept. LPMO, FEMTO-ST Besançon, France, e-mail `giordano@lpmo.edu`

5 Experimental Proof **10**
5.1 Noise Floor 10
5.2 Noise of an Attenuator 11
5.3 Low Noise Measurement 12

1 Introduction

For several reasons, some of which briefly considered underneath, phase noise plays a privileged rôle with respect to amplitude noise. In electronics, for instance, phase noise is generally integrated over a long time, while amplitude noise produces local effects only. Then, digital circuits are relatively immune to amplitude noise but prone to transition jitter, which results from phase noise. Furthermore, the Barkhausen conditions for steady oscillation (unity gain and zero phase) impose that the internal phase fluctuations of an oscillator are transformed into frequency fluctuations; this results in enhanced phase fluctuations at the output of the oscillator [Lee66]. Finally, the frequency multiplication process also multiplies phase noise, which limits the maximum frequency attainable by frequency synthesis.

Phase noise is usually described in terms of the power spectrum density $S_\varphi(f)$ of the phase fluctuation $\varphi(t)$. In radiofrequency and microwave domain, up to 40 GHz or more, it is a common practice to measure $S_\varphi(f)$ by means of a fast Fourier transform (FFT) analyzer preceded by a phase to voltage converter consisting of a saturated mixer. In good experimental conditions and with relatively high carrier level, some 15 dBm, the sensitivity of a noise measurement system based on a saturated mixer can hardly be higher than -170 dBrad^2/Hz (white noise) plus -140 dBrad^2/Hz at $f = 1$ Hz (flicker). Higher sensitivity can be obtained by replacing the mixer with a radiofrequency interferometer, which shows lower noise and higher conversion gain. In this case, sensitivity is limited by the absolute temperature of the interferometer and by the noise figure of an amplifier, and therefore it is proportional to the carrier power P_o. For reference, with $P_o = 10$ dBm the noise floor can approach -180 dBrad^2/Hz.

The interferometric method was initially proposed as a means to characterize microwave amplifiers [San68]. Afterwards, it was used in conjunction with a discriminator for the measurement of the frequency stability of oscillators [Lab82]. More recently, this method was exploited for the measurement of the phase noise of X band passive devices [ITW97] and for the frequency stabilization of whispering gallery oscillators accomplished by dynamical phase noise correction [ITW96]. Then, a comprehension improvement [RGG99b] provided new design rules and the extension of the interferometric method to lower frequencies (100 MHz). Finally, the interferometer proved to be suitable to the measurement of the frequency stability of 5–10 MHz quartz resonators [RGBG00] with a sensitivity of some 10^{-14}.

On the other hand, the sensitivity of phase noise measurements can be improved by exploiting a correlation technique, in which two equal instruments simultaneously measure the same device. If the two instruments are indepen-

dent and only the device being tested is shared, the instrument noise is rejected. In frequency metrology, this technique was initially used as a means to measure the frequency stability of a Hydrogen maser pair [VMV64], and subsequently re-proposed in various ways [WSGG76, FGG83, Cur83, Wal92], with double balanced mixers as the phase detector.

Thus we combined the above two ideas, interferometer and correlation, proposing the double interferometer and implementing two prototypes [RGG98, RGG99a].

The noise floor of the double interferometer turns out to be limited by the temperature difference of the resistive terminations, instead of the absolute temperature. This noise compensation mechanism is similar to that of correlation radiometers and radio telescopes. But our instrument is designed to measure the power spectrum density of noise close to a strong carrier signal, say 0 to 20 dBm, instead of the power of small radiation alone. A noise floor of some -195 $\mathrm{dBrad}^2/\mathrm{Hz}$ can be attained with a carrier power below 10 dBm.

The double interferometer, although originally intended as a means to characterize components for high stability oscillators, is actually a tool for general experiments involving the measurement of low noise phenomena in the vicinity of a strong carrier signal. In addition, as the double interferometer removes the thermal floor, it makes possible the measurement of flicker noise at higher Fourier frequencies than other instruments.

2 Basic Concepts

A high signal-to-noise ratio sinusoidal signal $s(t)$ of frequency ν_0 and power P_o at the output of a source impedance matched to its characteristic impedance R_0 can be represented as

$$s(t) = \sqrt{2R_0P_o}\ [1+\alpha(t)]\ \sin\left[2\pi\nu_0 t + \varphi(t)\right] \quad . \tag{1}$$

$\varphi(t)$ and $\alpha(t)$ are the phase modulation (PM) noise and the amplitude modulation (AM) noise, respectively. The physical quantity of major interest is the power spectrum density (PSD) $S_\varphi(f)$ of $\varphi(t)$ as a function of the Fourier frequency f.

The signal (1) can be rewritten as

$$s(t) = \sqrt{2R_0P_o}\ \sin\ [2\pi\nu_0 t] + n(t) \quad , \tag{2}$$

where $n(t)$ is the random voltage that causes AM and PM noise. Then, $n(t)$ can be divided as

$$n(t) = n_c(t)\cos(2\pi\nu_0 t) + n_s(t)\sin(2\pi\nu_0 t) \quad , \tag{3}$$

which is related to the AM and PM noise by

$$\alpha(t) = \frac{n_s(t)}{\sqrt{R_0P_o}} \qquad \text{and} \qquad \varphi(t) = \frac{n_c(t)}{\sqrt{R_0P_o}} \quad . \tag{4}$$

The spectrum densities $N_c(f)$ and $N_s(f)$ come from the superposition of the upper and lower sidebands of $n(t)$, i.e. $N(\nu_0+f)$ and $N(\nu_0-f)$, which is inherent in the frequency conversion process.

If $n(t)$ is a true additive random voltage, like thermal noise is, $n_c(t)$ and $n_s(t)$ are independent random variables of equal PSD. We assume that even if $n(t)$ is of parametric origin, $n_c(t)$ and $n_s(t)$ are independent, although their PSDs may be different. In most cases, this approximation is close to the actual behavior of radiofrequency and microwave devices. In fact, in the presence of a carrier signal the noise phenomena of these devices tend to affect phase and amplitude independently. Moreover, $n(t)$ can be represented as $n(t) = n^{\rm th}(t) + n^{\rm ex}(t)$, which is the superposition of thermal noise $n^{\rm th}(t)$ and extra noise $n^{\rm ex}(t)$; we use the word "extra" to avoid "excess" because the latter is often considered synonymous of flicker, which is more restrictive. Obviously, AM and PM noise, as well as spectra, can be divided in the same way. Furthermore, we assume that $n^{\rm th}(t)$ and $n^{\rm ex}(t)$ are independent. Finally, $n^{\rm th}(t)$ and $n^{\rm ex}(t)$ can be separately decomposed according to (3).

As a consequence of the Nyquist theorem, a resistor of value R_0 at temperature T can be modeled with a cold resistor R_0 in series to a generator of random voltage $2\,n(t)$ that accounts for thermal noise. Hence, a voltage $n(t)$ is available across an impedance matched load. The corresponding PSD is $N(\nu) = k_B T R_0$, where $k_B = 1.38\times10^{-23}$ is Boltzmann constant. With thermal noise, it holds $N_c(f) = k_B T R_0$ and $N_s(f) = k_B T R_0$. Thus, a sinusoidal signal from a source whose internal resistance is at temperature T is affected by AM noise $S_\alpha^{\rm th}(f) = k_B T/P_o$ and by PM noise $S_\varphi^{\rm th}(f) = k_B T/P_o$.

The extension of the Nyquist theorem for circuits at nonuniform temperature yields the description of the attenuator behavior shown in Fig. 1. The attenuator, of power loss ℓ, is impedance matched to R_0 at both ends, and is at temperature T_a. When the thermal noise $n_i(t)$ from a resistance R_0 at temperature T_i crosses this attenuator, it results in a random signal $n'_o(t) = n_i(t)/\sqrt{\ell}$ at the output. The attenuator adds its noise. Indicating with $n_a(t)$ the equivalent noise voltage of a resistance R_0 at the temperature T_a, the noise contribution of the attenuator is $n''_o(t) = \sqrt{(1-\ell)/\ell}\, n_a(t)$. This is related to the fact that if the attenuator and the resistor are at the same temperature T the total output spectrum density $N_o(\nu) = N'_o(\nu) + N''_o(\nu)$ must be equal to $k_B T R_0$ and independent of ℓ, and that for $\ell = \infty$ the equivalent temperature observed at the output is T_a.

Let us now consider the sum and the difference of two independent random signals $n_1(t)$ and $n_2(t)$

$$a(t) = \frac{1}{\sqrt{2}}\Big[n_1(t) + n_2(t)\Big] \tag{5}$$

$$b(t) = \frac{1}{\sqrt{2}}\Big[n_1(t) - n_2(t)\Big] \ , \tag{6}$$

obtained either as the result of a mere algebraic operation or by means of a lossless 3 dB coupler; such a coupler, that does not add thermal noise, is the

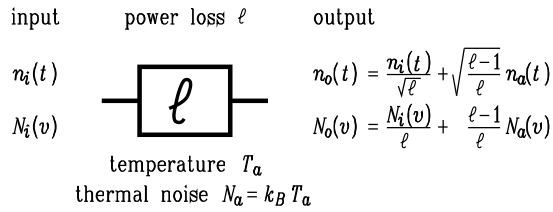

Figure 1: Noise model of an attenuator.

idealization of a 3 dB hybrid junction, i.e., a transformer, a microstrip network or a microwave magic T. As we need not a representation of form (1) or (3), we can use the baseband frequency f, which is consistent with the notation of Section 4. The cross PSD of $a(t)$ and $b(t)$ is, by definition,

$$S_{ab}(f) \;=\; \mathcal{F}\left\{\mathcal{R}_{ab}(\tau)\right\} \;=\; \int_{\infty} \mathcal{R}_{ab}(\tau)\exp(-2\pi f\tau)\,\mathrm{d}\tau \quad , \tag{7}$$

where $\mathcal{F}\{.\}$ is the Fourier transform operator, and $\mathcal{R}_{ab}(\tau)$ is the cross correlation function

$$\mathcal{R}_{ab}(\tau) = \lim_{\theta\to\infty} \frac{1}{\theta}\int_{\theta} a(t)\, b^*(t-\tau)\,\mathrm{d}t \quad ; \tag{8}$$

the symbol "$*$" stands for complex conjugate and can be omitted because we deal with real signals. Making $n_1(t)$ and $n_2(t)$ appear in (7), and dividing thermal and extra noise, we get

$$S_{ab}(f) \;=\; \frac{1}{2}\Big[N_1(f) - N_2(f)\Big] \tag{9}$$

$$\;=\; \frac{1}{2}\Big[k_B\,(T_1 - T_2)\,R_0 + N_1^{\mathrm{ex}}(f) - N_2^{\mathrm{ex}}(f)\Big] \quad . \tag{10}$$

This means that, if $n_2(t)$ is a pure thermal fluctuation and the temperature of the instrument is homogeneous ($T_1 = T_2$), the instrument compensates for thermal noise and measures the extra noise $N_1^{\mathrm{ex}}(f)$ only. Alternatively, in the absence of extra noise, the instrument noise floor is limited by the temperature inhomogeneity $T_1 - T_2$.

$S_{ab}(f)$ is related to the Fourier transform $A(f)$ and $B(f)$ of the individual signals by

$$S_{ab}(f) = A(f)\,B^*(f) \quad . \tag{11}$$

Generally, dynamic signal analyzers make use of (11) replacing the true Fourier transform with the FFT of $a(t)$ and $b(t)$ simultaneously sampled, and averaging over m acquisitions. Thus, the estimate of the spectrum $S_{ab}(f)$ is affected by a rms uncertainty

$$\sigma_{S_{ab}} = \frac{|A|\,|B|}{\sqrt{2m}} \quad . \tag{12}$$

If $a(t)$ and $b(t)$ are uncorrelated, the estimate of $S_{ab}(f)$ approaches zero proportionally to $1/\sqrt{2m}$, being limited by the uncertainty (12). Therefore, a long averaging time may be needed to attain the ultimate noise floor of the instrument, determined by temperature inhomogeneity or crosstalk.

It should be remarked that the high sensitivity of the correlation microwave radio telescopes [Blu59, Kra66] relies upon (10). A similar mechanism is exploited in the Allred radiometer [All62, AAC64] to compare a noise source to a reference one. This instrument works as a sort of bridge that is nulled observing the sign of S_{ab} and controlling the reference source. The noise compensation mechanism (10), combined with a carrier suppression technique and down conversion, makes the realization of our high sensitivity phase noise measurements system possible.

3 The Phase Noise Measurement System

The theory of the interferometer is reported in [RGG99b], together with design strategies and experimental results. The double interferometer, shown in Fig. 2, consists of two interferometers that simultaneously measure the phase noise of single device under test (DUT). Setting the variable attenuators ℓ and the variable phase shifters γ' equal to the DUT phase and attenuation, all the oscillator power goes to the Σ port of the hybrids, while the carrier is suppressed at the Δ outputs. The carrier suppression mechanism has no effect on the DUT noise. Therefore, one-fourth of the power of the DUT noise sidebands is present at the input of each amplifier. Setting the phases γ'' equal to the phase lag of the amplifiers, the mixers down convert the DUT phase noise to baseband. In this condition, the voltages $a(t)$ and $b(t)$ present at the output of the mixers are proportional to the instant value of the DUT phase $\varphi(t)$. Consequently, the cross PSD of the two output signals is proportional to the DUT phase noise PSD, while the individual interferometer noise is rejected.

The three hybrids on the left part of Fig. 2 are used as power splitters and may be replaced with them. It should be remarked that the power splitter is actually a 4 port hybrid internally terminated at one port, otherwise it could not be impedance matched at all ports. The scheme of Fig. 2 is based on 90° hybrids, which corresponds to the 100 MHz implementation used in this paper. Yet, any other combination of 180° and 90° hybrids and power splitters would work in the same way. The only constraint is that the carrier suppression and the detection of the DUT phase noise must be ensured by properly setting γ' and γ''.

4 Signal Analysis of the Double Interferometer

Let us now analyze in detail the double interferometer set up for the measurement of a generic DUT of loss ℓ that produces both thermal and extra noise.

As the oscillator provides the phase reference to the whole machine, its

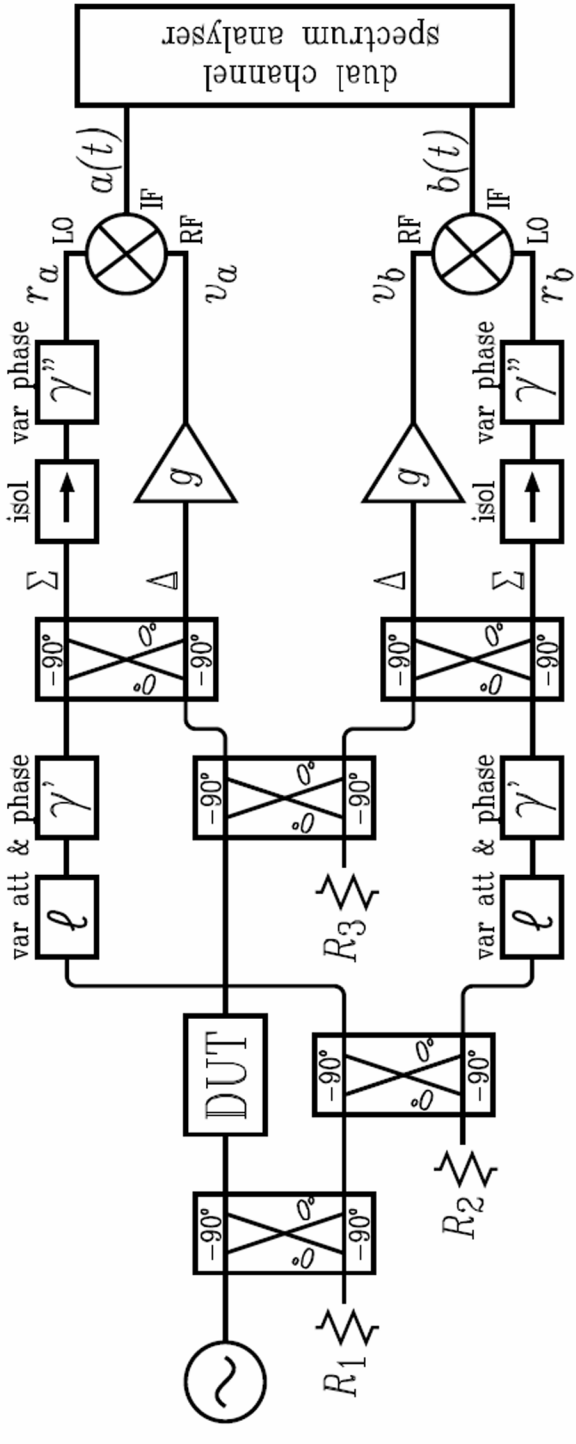

Figure 2: Scheme of the double interferometer.

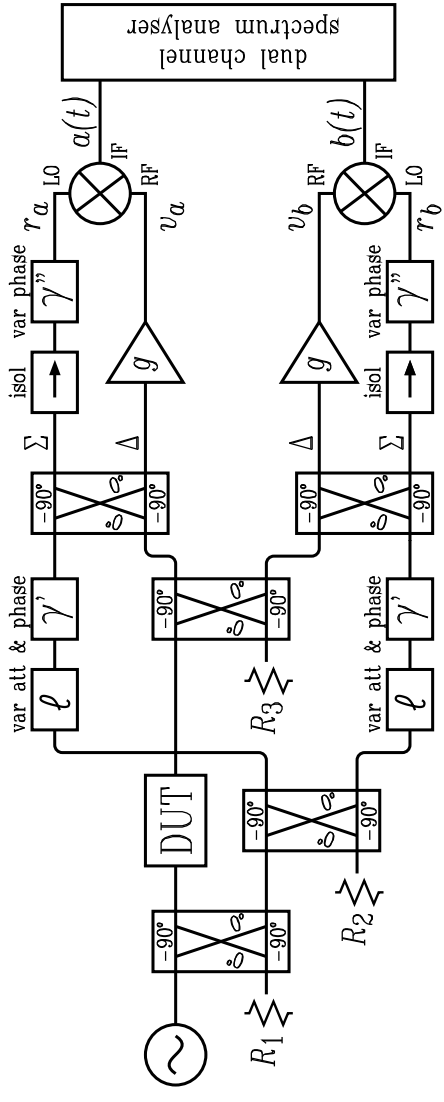

Figure 2: Scheme of the double interferometer.

phase noise is rejected. The noise of the variable attenuators and phase shifters responsible for the carrier suppression vanishes in the correlation and averaging process because these devices are independent and the two arms are isolated. The noise of the two amplifiers vanishes for the same reason. The mixers and the detection phase shifters γ'' are independent and they process amplified signals, thus their noise contribution is negligible. At a deeper sight, one can observe that the effect of all the independent noise sources (attenuators, phase shifters, amplifiers etc.) can only be an increase in the number m of averages needed

for a given noise floor, according to (12). For the sake of simplicity, we assume that the hybrids are lossless and noiseless; anyway, non-ideality of the hybrids can be reintroduced later in the equations.

Under the above assumptions, there remain four random signals shared by the two arms, namely the DUT noise $n_d(t)$ and the thermal noise $n_1(t)$, $n_2(t)$ and $n_3(t)$ of the resistive terminations R_1, R_2 and R_3 at temperature T_1, T_2 and T_3; as there is no ambiguity, we omit the superscript 'th' of $n_1(t)$, $n_2(t)$ and $n_3(t)$. Defining the thermal noise of a resistor at temperature T_d as $n_d^{\rm th}(t)$, the model of Fig. 1 yields a DUT noise contribution of $\sqrt{(\ell-1)/\ell}\; n_d^{\rm th}(t)$. Besides this, we define the extra noise at the DUT output as $n_d^{\rm ex}(t)$.

When the oscillator signal $\sqrt{2R_0P_r}\cos(2\pi\nu_0 t)$ is taken as the phase reference, the phase of the DUT output signal is that of $\sin(2\pi\nu_0 t)$. Hence, phase noise comes from the $n_c(t)\cos(2\pi\nu_0 t)$ component of the DUT noise. Consequently, it holds $S_\varphi(f) = N_c(f)/(R_0P_o)$, where P_o is the carrier power at the DUT output.

The reference signals at the mixer LO ports are

$$r_a(t) = -V_p\,\cos(2\pi\nu_0 t) \tag{13}$$

$$r_b(t) = V_p\,\sin(2\pi\nu_0 t)\ . \tag{14}$$

Accordingly, arm a detects the $\cos(2\pi\nu_0 t)$ component of the signal present at the RF port of the mixer, and arm b detects the $\sin(2\pi\nu_0 t)$ component. These RF signals are

$$\begin{aligned} v_a(t) = \sqrt{g}\Bigg[&-\frac{1}{\sqrt{2\ell}}\,n_{1c}(t)+\frac{1}{2\sqrt{\ell}}\,n_{2c}(t)+\frac{1}{2}\,n_{3s}(t)+\\ &-\frac{1}{2}\sqrt{\frac{\ell-1}{\ell}}\,n_{d\,c}^{\rm th}(t)-\frac{1}{2}\,n_{d\,c}^{\rm ex}(t)\Bigg]\cos(2\pi\nu_0 t)\ +\\ &+\sqrt{g}\left[\begin{array}{c}\text{non}\\ \text{detected}\\ \text{terms}\end{array}\right]\sin(2\pi\nu_0 t) \end{aligned} \tag{15}$$

$$\begin{aligned} v_b(t) = \sqrt{g}\Bigg[&\frac{1}{\sqrt{2\ell}}\,n_{1c}(t)+\frac{1}{2\sqrt{\ell}}\,n_{2c}(t)+\frac{1}{2}\,n_{3s}(t)\ +\\ &+\frac{1}{2}\sqrt{\frac{\ell-1}{\ell}}\,n_{d\,c}^{\rm th}(t)+\frac{1}{2}\,n_{d\,c}^{\rm ex}(t)\Bigg]\sin(2\pi\nu_0 t)\ +\\ &+\sqrt{g}\left[\begin{array}{c}\text{non}\\ \text{detected}\\ \text{terms}\end{array}\right]\cos(2\pi\nu_0 t)\ . \end{aligned} \tag{16}$$

After filtering out the $2\nu_0$ components, the down converted signals are

$$\begin{aligned} a(t) = \sqrt{\frac{2g}{\ell_m}}\Bigg[&\frac{1}{\sqrt{2\ell}}\,n_{1c}(t)-\frac{1}{2\sqrt{\ell}}\,n_{2c}(t)-\frac{1}{2}\,n_{3s}(t)+\\ &+\frac{1}{2}\sqrt{\frac{\ell-1}{\ell}}\,n_{d\,c}^{\rm th}(t)+\frac{1}{2}\,n_{d\,c}^{\rm ex}(t)\Bigg] \end{aligned} \tag{17}$$

$$
\begin{aligned}
b(t) &= \sqrt{\frac{2g}{\ell_m}} \left[\frac{1}{\sqrt{2\ell}}\, n_{1c}(t) + \frac{1}{2\sqrt{\ell}}\, n_{2c}(t) + \frac{1}{2}\, n_{3s}(t) + \right. \\
&\quad \left. + \frac{1}{2}\sqrt{\frac{\ell-1}{\ell}}\, n^{\rm th}_{d\,c}(t) + \frac{1}{2}\, n^{\rm ex}_{d\,c}(t) \right] \quad , \qquad (18)
\end{aligned}
$$

where ℓ_m is the mixer loss; according to the usual definition, ℓ_m includes the 3 dB intrinsic loss due to the fact that the mixer makes the sum and the difference of its input frequencies, and consequently it splits the input power into two bands.

The cross correlation $\mathcal{R}_{ab}(\tau)$ contains only the autocorrelation terms, while the mixed ones vanish because all the noise processes are independent. Hence, the cross PSD is

$$
\begin{aligned}
S_{ab}(f) &= \frac{g}{\ell_m} \left[\frac{1}{\ell}\, N_{1c}(f) - \frac{1}{2\ell}\, N_{2c}(f) - \frac{1}{2}\, N_{3s}(f) \; + \right. \\
&\quad \left. + \frac{\ell-1}{2\ell}\, N^{\rm th}_{d\,c}(f) + \frac{1}{2}\, N^{\rm ex}_{d\,c}(f) \right] \qquad (19)
\end{aligned}
$$

and therefore

$$
\begin{aligned}
S_{ab}(f) &= \frac{g k_B}{\ell_m} \left[\frac{1}{\ell}\, T_1 - \frac{1}{2\ell}\, T_2 - \frac{1}{2}\, T_3 + \frac{\ell-1}{2\ell}\, T_d \right] + \\
&\quad + \frac{g}{2\ell_m}\, N^{\rm ex}_{d\,c}(f) \quad . \qquad (20)
\end{aligned}
$$

If the whole machine is at the same temperature $T = T_0$, the cross PSD reduces to

$$
S_{ab}(f) = \frac{g}{2\ell_m}\, N^{\rm ex}_{d\,c}(f) \quad , \qquad (21)
$$

which is determined by the DUT extra noise only. Therefore, under the hypothesis of temperature uniformity, only the extra noise $N^{\rm ex}_{d\,c}(f)$ contributes to the observed spectrum. This means that the simple noise compensation mechanism given by (10) also takes place in the double interferometer, making the thermal noise vanish.

To derive the gain $K_\varphi = S_{ab}(f)/S_\varphi(f)$ of the double interferometer we assume that thermal noise is negligible compared to the DUT extra noise, i.e. $N_d(f) \simeq N^{\rm ex}_d(f)$. Then, inserting $S_\varphi(f) = N_c(f)/(R_0 P_o)$ in (21) we get

$$
K_\varphi = \frac{g R_0 P_o}{2\ell_m} \quad . \qquad (22)
$$

As there are two hybrids along the signal path from the DUT to the amplifier, each of which shows a loss ℓ_h, actual gain is lower than (22) by a factor $1/\ell_h^2$.

The single-arm noise floor $S_{\varphi\,0}(f)$ can be derived from the equivalent noise $F k_B T_0$ at the amplifier input, where F is the amplifier noise figure. The PSD of the down converted voltage, either $a(t)$ or $b(t)$, is $S_{v\,0}(f) = 2 F g k_B T_0 R_0/\ell_m$. Dividing the latter by the gain (22), we get

$$
S_{\varphi\,0}(f) = 4\, \frac{F k_B T_0}{R_0 P_o} \quad . \qquad (23)
$$

Then, accounting for the hybrid loss, actual noise floor is higher than (23) by a factor ℓ_h^2.

Finally, the double interferometer can be set up to detect amplitude noise. This is easily accomplished by adding 90° to the two phase shifters γ'', which causes the $n_s(t)$ component of the DUT noise to be down converted instead of the $n_c(t)$ one. Equations (16) to (23) still hold, provided some obvious subscript changes were done.

5 Experimental Proof

5.1 Noise Floor

We measured the noise floor of a double interferometer prototype designed for the carrier frequency $\nu_0 = 100$ MHz. To do so, the DUT is replaced with a short cable, which is noiseless. In this prototype, the hybrids show a loss $\ell_h = 0.8$ dB, while the loss of the mixers is $\ell_m = 6$ dB. The signal power at the mixer LO inputs is 8 dBm, and the DUT power is $P_o = 8$ dBm. The amplifiers show a gain $g = 40$ dB, a noise figure $F = 2$ dB, and a bandwidth of some 30 MHz centered around ν_0. All the circuit is impedance matched to $R_0 = 50\ \Omega$. Further details of this instrument are reported in [RGG99a].

Properly adjusting the interferometers, the carrier suppression is at least 65 dB. In this condition, the amplifier linearity is ensured because the residual output carrier never exceeds -25 dBm, which is 40 dB lower than the 1 dB compression point of the amplifiers.

In order to set the phases γ'' for the two mixers to detect phase noise, the DUT is replaced with a small-angle phase modulator driven by the oscillator output of a lock-in. Thus, a sinusoidal modulation of the order of 1 mrad is injected. Then, each phase shifter is adjusted for zero voltage at the output of the corresponding mixer, which is measured with the lock-in. Finally, two 90° cables calibrated by means of a network analyzer are added to γ''. Due to the high sensitivity of the described null method, phase accuracy and phase matching of the order of 1° can easily be obtained. The phase modulator and the lock-in are also used to measure the gain K_φ, which is 24.5 $\mathrm{dBV}^2/\mathrm{rad}^2$ in this case.

The rejection of the driving oscillator noise turns out to be higher than 60 dB in the described conditions. Using a low noise quartz oscillator that exhibits a floor of -157 $\mathrm{dBrad}^2/\mathrm{Hz}$, the noise contribution of that oscillator is negligible for our purposes.

Fig. 3 shows the results averaged on $m = 32767$ measures, which is the maximum of the available spectrum analyzer. Flicker and acoustic vibrations appear in the left part of the plot, while for $f \geq 2$ kHz white noise only is present. The single-arm noise floor (curves A and B) is -172 $\mathrm{dBrad}^2/\mathrm{Hz}$, which is close to the expected value $S_{\varphi 0}(f) = 4Fk_BT_0\ell_h^2/P_o \simeq -172.3$ $\mathrm{dBrad}^2/\mathrm{Hz}$. For reference, the thermal noise of a resistor at $T_0 = 290$ K referred to the same carrier power P_o is $S_\varphi^{\mathrm{th}}(f) = k_BT_0/P_o \simeq -182$ $\mathrm{dBrad}^2/\mathrm{Hz}$. Yet, the cross

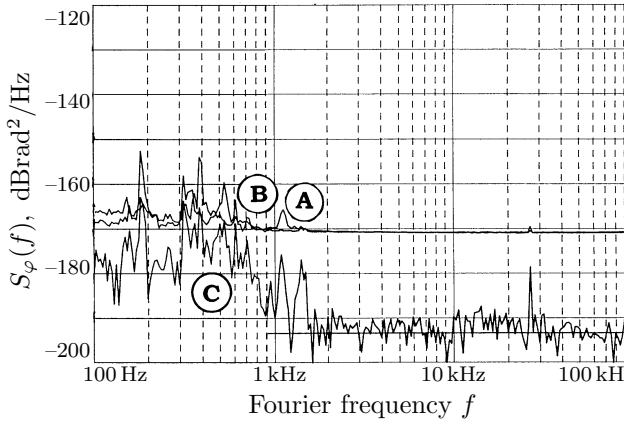

Figure 3: Noise floor of the 100 MHz double interferometer prototype. A and B: single-arm. C: correlation.

spectrum floor (curve C) is -194 dBrad^2/Hz, which is 12 dB lower than the thermal floor $S_\varphi^{\mathrm{th}}(f)$.

As a consequence of (12), a rms uncertainty $S_{\varphi 0}/\sqrt{2m} \simeq -196$ dBrad^2/Hz is expected, which is close to the observed floor. Consequently, that floor is due to the insufficient averaging capability of the analyzer instead of a true hardware limitation, and it is expected to further decrease, increasing m.

5.2 Noise of an Attenuator

The analytical development of equation (21) predicts that the thermal noise of an attenuator of loss ℓ inserted as the DUT vanishes in the correlation-and-averaging process if the temperature of the whole machine is uniform, and that this is independent of ℓ. We demonstrate this fact through an experiment in which a three port device (that also includes the hybrid present in the center of Fig. 2) is measured, comparing the two configuration of Fig. 4. In A, most of the output noise comes from the two independent $\ell = 16$ dB attenuators, while in B there is only one $\ell = 16$ dB attenuator along the shared path. Yet, the cross PSD is expected to approach zero in both cases.

All the experimental conditions are the same for the two configurations, except for the detail of Fig. 4. Thus, the hybrid driving power is different, but this is not relevant because the hybrid is not power-sensitive. Moreover, we choose a device specified for continuous operation up to 36 dBm, while the input power does not exceed 22 dBm. The oscillator power is $P_r = 26$ dBm. Accordingly, the output power is $P_o = 6$ dBm at each port, the same for both configurations. All other circuit parameters, as well as the adjustment and calibration, are the same as described in Section 5.1.

The measured PSDs, averaged on $m = 1024$ measures, are shown in Fig. 5.

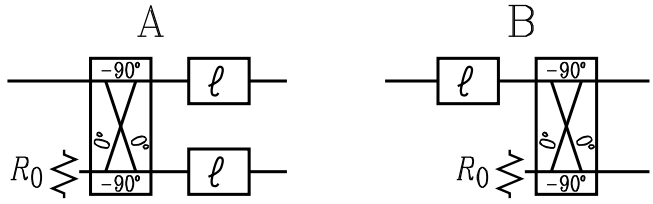

Figure 4: Measurement schemes with the 16 dB attenuators.

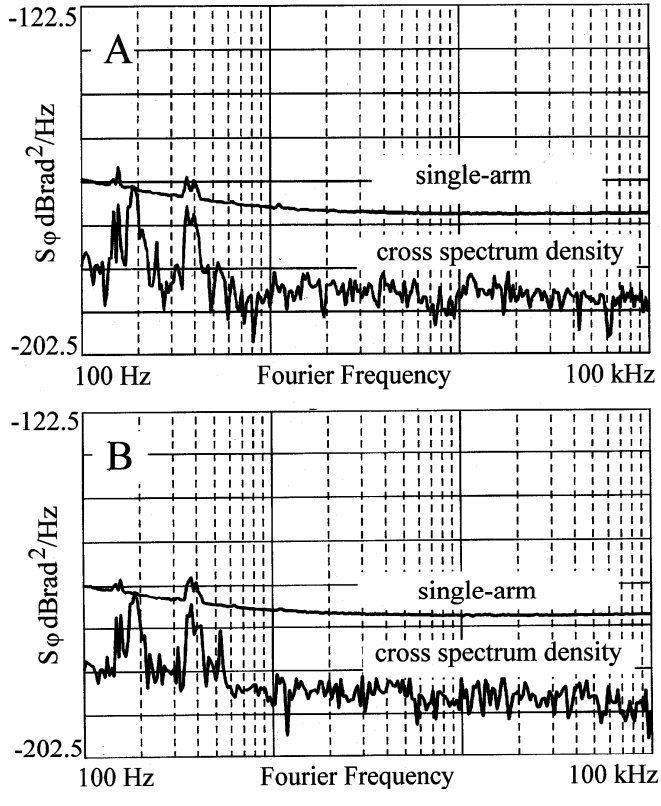

Figure 5: Phase noise measured with the two 16 dB attenuator configurations.

We focus our attention on the white noise floor, for $f > 1$ kHz. According to (23), the expected single-arm noise is $S_{\varphi\,0}(f) = -170.4$ dBrad^2/Hz, which is experimentally confirmed with both configurations.

The cross PSD floor is -187 dBrad^2/Hz, almost equal for both configurations. That floor is lower than the thermal energy referred to the carrier power, i.e. $S_\varphi^{\rm th} = k_B T_0/P_o = -182$ dBrad^2/Hz, and corresponds to the uncertainty limit given by (12).

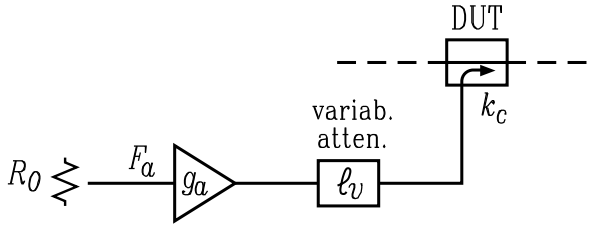

Figure 6: Injection of the reference noise N_d^{ex}.

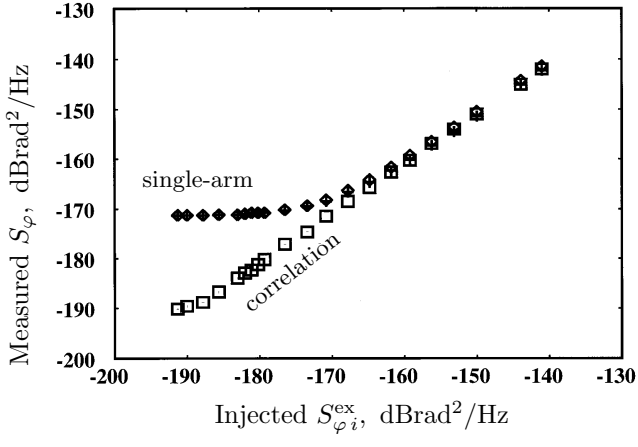

Figure 7: Reference noise measurement.

5.3 Low Noise Measurement

The DUT is now replaced with the circuit shown in Fig. 6, which enables the injection of extra noise $N_d^{\text{ex}}(\nu) = g_a R_0 F_a k_B T_0/(\ell_v k_c)$ through a directional coupler. This corresponds to a phase noise $S_{\varphi i}^{\text{ex}} = g_a R_0 F_a k_B T_0/(\ell_v k_c P_o)$, plus an amplitude noise of the same value; the latter is negligible because it is not detected. The source PSD is $F_a k_B T_0 g_a \simeq -100.5$ dBm/Hz, while the coupling factor is $k_c = 11.5$ dB. The attenuator consists of a 0 to 70 dB variable unit in series to a 20 dB fixed one; for best impedance matching and stability, the fixed attenuator is located close to the directional coupler. As the DUT power is $P_o = 8$ dBm, the injected extra noise can be set to the desired value in the -140 to -210 dBrad^2/Hz range. In addition, the presence of thermal noise is ensured by impedance matching. The usefulness of this arrangement consists of the capability of calibrating a sub-thermal random signal by means of relatively large signal measurements only, which can be easily performed with conventional spectrum and network analyzers.

All the operating parameters of this experiment are the same as those reported in Section 5.1 except for m, that is reduced when possible.

Fig. 7 shows the measured floor $S_{\varphi\,0}$ averaged over f from some 5 to 50 kHz, as a function of the injected $S^{\rm ex}_{\varphi\,i}$. Going towards the left of that figure, ℓ_v increases and the injected noise becomes negligible compared to the single-arm noise floor. Therefore, the single-arm phase noise approaches the $S_{\varphi\,0} = -172$ dBrad^2/Hz, the same value that was measured in the absence of the DUT. By contrast, the correlated noise fits the straight line $S_\varphi = S^{\rm ex}_{\varphi\,i}$. Consequently, still under the hypothesis of temperature uniformity, the instrument compensates for the thermal noise and measures the extra noise only. This confirms what we expect from equation (21).

Acknowledgments

We wish to acknowledge Michele Elia from the Politecnico di Torino for having greatly contributed to the theoretical comprehension of our experiments, and Marcel Olivier and Jacques Groslambert from the LPMO for their support and for valuable scientific discussions.

References

[AAC64] M. G. Arthur, C. M. Allred, and M. K. Cannon, *A precision noise power comparator*, IEEE Trans. Instrum. Meas. **13** (1964), 301–305. 2

[All62] C. M. Allred, *A precision noise spectral density comparator*, J. Res. NBS **66C** (1962), 323–330. 2

[Blu59] E. J. Blum, *Sensibilité des radiotelescopes et recepteurs à correlation*, Ann. Astrpohysique **22** (1959), no. 2, 140–163. 2

[Cur83] G. S. Curtis, *The relationship between resonator and oscillator noise and resonator noise measurement technique*, Proc. Freq. Control Symp. (Philadelphia, PA, USA), June 1-3 1983, pp. 218–225. 1

[FGG83] D. Fest, J. Groslambert, and J. J. Gagnepain, *Individual characterization of an oscillator by means of cross-correlation or cross covariance method*, IEEE Trans. Instrum. Meas. **32** (1983), no. 3, 447–450. 1

[ITW96] Eugene N. Ivanov, Michael E. Tobar, and Richard A. Woode, *Ultra-low noise microwave oscillator with advanced phase noise suppression system*, Microw. Guided Wave Lett. **6** (1996), no. 9, 312–315. 1

[ITW97] ———, *A study of noise phenmena in microwave components using an advanced noise measurement system*, IEEE Trans. Ultras. Ferroel. and Freq. Contr. **44** (1997), no. 1, 161–163. 1

[Kra66] J. D. Kraus, *Radio astronomy*, McGraw Hill, New York, 1966. 2

[Lab82] F. Labaa, *New discriminator boosts phase noise testing*, Microwaves **21** (1982), no. 3, 65–69. 1

[Lee66] D. B. Leeson, *A simple model of feed back oscillator noise spectrum*, Proc. IEEE **54** (1966), 329–330. 1

[RGBG00] Enrico Rubiola, Jacques Groslambert, Michel Brunet, and Vincent Giordano, *Flicker noise measurement of HF quartz resonators*, IEEE Trans. Ultras. Ferroel. and Freq. Contr. **47** (2000), no. 2, 361–368. 1

[RGG98] Enrico Rubiola, Vincent Giordano, and Jacques Groslambert, *Double correlating interferometer scheme to measure PM and AM noise*, Electron. Lett. **34** (1998), no. 1, 93–94. 1

[RGG99a] ———, *Improved interferometric method to measure near-carrier AM and PM noise*, IEEE Trans. Instrum. Meas. **48** (1999), no. 2, 642–646. 1, 5.1

[RGG99b] ———, *Very high frequency and microwave interferometric PM and AM noise measurements*, Rev. Sci. Instrum. **70** (1999), no. 1, 220–225. 1, 3

[San68] K. H. Sann, *The measurement of near-carrier noise in microwave amplifiers*, IEEE Trans. Microw. Theory Tech. **9** (1968), 761–766. 1

[VMV64] R. F. C. Vessot, R. F. Mueller, and J. Vanier, *A cross-correlation technique for measuring the short-term properties of stable oscillators*, Proc. IEEE-NASA Symposium on Short Term Frequency Stability (Greenbelt, MD, USA), November 23-24 1964, pp. 111–118. 1

[Wal92] W. F. Walls, *Cross-correlation phase noise measurements*, Proc. Freq. Control Symp. (Hershey, PA), IEEE, New York, 1992, May 27-29 1992, pp. 257–261. 1

[WSGG76] F. L. Walls, S. R. Stain, J. E. Gray, and D. J. Glaze, *Design considerations in state-of-the-art signal processing and phase noise measurement systems*, Proc. Freq. Control Symp. (Atlantic City, NJ, USA), EIA, Washington, DC, 1965, June 2-4 1976, pp. 269–274. 1